Electron-Transfer-Coupled Ligand Dynamics in $Cu^{I/II}(TTCN)_2$ Complexes in Aqueous Solution

Sanaullah,[†] Hartmut Hungerbühler,[‡] Christian Schöneich,[§] Martha Morton,[†] David G. Vander Velde,[†] George S. Wilson,*[,†] Klaus-Dieter Asmus,*[,∥] and Richard S. Glass*[,⊥]

Contribution from the Departments of Chemistry and Pharmaceutical Chemistry, The University of Kansas, Lawrence, Kansas 66045, Bereich Physikalische Chemie, Abteilung Strahlenchemie, Hahn-Meitner Institut Berlin, Glienicker Strasse 100, 14109 Berlin, Germany, Radiation Laboratory and Department of Chemistry and Biochemistry, University of Notre Dame, Notre Dame, Indiana 46556, and the Department of Chemistry, The University of Arizona, Tucson, Arizona 85721

Received August 8, 1996[⊗]

Abstract: One-electron oxidation of copper(I) bis(1,4,7-trithiacyclononane), $[Cu^{I}(TTCN\text{-}\kappa^3)(TTCN\text{-}\kappa^1)]^+$, **1**, a coordination complex with a tetrahedral CuS_4 core, to $[Cu^{II}(TTCN\text{-}\kappa^3)_2]^{2+}$, **2**, with an octahedral CuS_6 core, has been studied by pulse radiolysis and electrochemistry in aqueous solution at various pH values. In addition to the geometry change about the metal ion in this oxidation, the nonchelating 1,4,7-trithiacyclononane (TTCN) ligand in **1** changes conformation on becoming chelated in **2**. However, pulse radiolysis reveals that this process does not occur intramolecularly but affords a bimolecular reaction in which the oxidized copper incorporates an external TTCN. Evidence for this mechanism is drawn from corresponding experiments with a variety of related Cu^{I} complexes in which the monodentate TTCN has been replaced by other sulfur-containing ligands and which have been structurally characterized by X-ray crystallography. From all these studies it is concluded that oxidation of **1** and all these other complexes of Cu^{I} is accompanied by immediate loss of the monodentate ligand generating $[Cu^{II}(TTCN\text{-}\kappa^3)(H_2O)_3]^{2+}$, **3**. Transient **3** is characterized by an optical absorption with $\lambda_{max} = 370$ nm and $\epsilon \sim 2000\ M^{-1}\ cm^{-1}$ which depends on pH because this transient participates in three acid/base equilibria. Deprotonation of the three water ligands associated with Cu(II) results in increasingly blue-shifted absorptions. Undeprotonated transient **3** prevails at pH $\leq$6, and converts directly into the stable Cu^{II} complex **2** via reaction with an unoxidized molecule of **1** or free TTCN. The corresponding bimolecular rate constants are 5.2 ($\pm$0.5) $\times 10^5$ and 8.4 ($\pm$1.0) $\times 10^5\ M^{-1}\ s^{-1}$, respectively. For the deprotonated forms of **3** this process is increasingly slowed down and at higher pH ($\geq$9) the formation of **2** is completely prevented. The formation of transient **3** is also consistent with the pH dependence of the electrochemistry of **1**. Under electrochemical conditions the conversion into **2** follows first-order kinetics due to a relatively high TTCN concentration available near the electrode surface after oxidation of **1**. All the results require rapid ligand exchange in **1** and a particularly labile monodentate TTCN ligand. This has been corroborated by ^1H NMR spectroscopic studies on **1**.

Introduction

The redox chemistry of $Cu^{I/II}$ is intriguing because there is a change in coordination geometry associated with the change in oxidation state: d^{10} Cu^{I} is preferentially tetrahedral and d^9 Cu^{II} typically adopts tetragonal or square-planar geometry.[1] The role of ligated protein and copper ion coordination geometries is important in copper-containing redox proteins.[2,3] For example, the key to the remarkable properties of "blue" copper proteins[4,5] may be the distorted geometries of the metal center, involving (2N, 2S) donor sets, which is intermediate between the preferred Cu^{I} and Cu^{II} coordination geometries.[5]

The redox chemistry of $[Cu^{I/II}(TTCN)_2]$ presents a fascinating system for detailed studies because the change in oxidation state of the copper ion is accompanied by substantial geometric changes in the coordination sphere of the metal ion as well as one of the ligands. The conformation and coordination versatility of the 1,4,7-trithiacyclononane (TTCN) ligand shown in Figure 1 has resulted in a large variety of transition metal complexes with novel structural, spectroscopic, and redox properties.[6,7] While the TTCN-κ^3 ligand in $[Cu^{I}(TTCN\text{-}\kappa^3)(TTCN\text{-}\kappa^1)]^+$ (**1**; κ^n = *n*-dentate ligand),[8] shown in Figure 2, adopts the endodentate [333] conformation, found in the solid state for the free ligand,[9] the nonchelating TTCN-κ^1 has a unique conformation different from both the [333] and [12222][10]

[†] Department of Chemistry, The University of Kansas.
[‡] Hahn-Meitner Institut.
[§] Department of Pharmaceutical Chemistry, The University of Kansas.
[∥] University of Notre Dame.
[⊥] The University of Arizona.
[⊗] Abstract published in *Advance ACS Abstracts,* February 15, 1997.

(1) Cotton, F. A.; Wilkinson, G. *Advanced Inorganic Chemistry*, 5th ed.; Wiley: New York, 1988; pp 755−775.
(2) *Biological & Inorganic Copper Chemistry*; Karlin, K. D., Zubieta, J., Eds.; Adenine Press: Guilderland, NY, 1986; Vols. 1 and 2.
(3) *Bioinorganic Chemistry of Copper*; Karlin, K. D., Tyklár, Z., Eds.; Chapman & Hall: New York, 1993.
(4) Messerschmidt, A. *Adv. Inorg. Chem.* **1993**, *40*, 121.
(5) Kaim, W.; Schwederski, B. *Bioinorganic Chemistry: Inorganic Elements in the Chemistry of Life*; Wiley: Chichester, 1994; pp 187−214.
(6) Cooper, S. R.; Rawle, S. C. *Struct. Bonding (Berlin)* **1990**, *72*, 1.
(7) Blake, A. J.; Schröder, M. *Adv. Inorg. Chem.* **1990**, *35*, 1.
(8) Sanaullah; Kano, K.; Glass, R. S.; Wilson, G. S. *J. Am. Chem. Soc.* **1993**, *115*, 592.
(9) Glass, R. S.; Wilson, G. S.; Setzer, W. N. *J. Am. Chem. Soc.* **1980**, *102*, 5068.
(10) The [12222] conformation is adopted by the central, bridging TTCN molecule in $[Cu_2^{I}(TTCN)_3]$ (Clarkson, J. A.; Yagbasan, R.; Blower, P. J.; Cooper, S. R. *J. Chem. Soc., Chem. Commun.* **1989**, 1244) and the monodentate TTCN molecule in $[Cu^{I}(TTCN)_2]$ (Blake, A. J.; Gould, R. O.; Greig, J. A.; Holder, A. J.; Hyde, T. I.; Schroeder, M. *J. Chem. Soc., Chem. Commun.* **1989**, 876).

S0002-7863(96)02775-8 CCC: $14.00

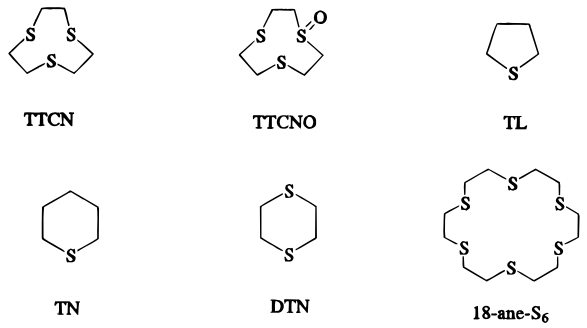

Figure 1. Drawings and labels of the ligands.

conformations. In $[Cu^{II}(TTCN\text{-}\kappa^3)_2]^{2+}$ (**2**),[11,12] shown in Figure 2, both TTCN ligands have the endodentate [333] conformation. The octahedral[11] or Jahn−Teller distorted[12] coordination geometry of the copper ion in **2** becomes tetrahedral in **1**.

In an effort to understand how these redox-associated geometry changes occur, the electrochemistry of this system has been studied in considerable detail.[8] Evidence was obtained for a chemical step which was fast on the CV time scale following electron transfer. The simplest interpretation of the data was an ECEC square mechanism[8,13,14] as shown in Scheme 1. In this proposal, oxidation of tetrahedral **1** first gives transient tetrahedral $[Cu^{II}(TTCN\text{-}\kappa^3)_2]^+$ which rearranges rapidly to octahedral **2** with an accompanying conformational change of one of the TTCN molecules. Reduction of octahedral **2**, on the other hand, affords transient octahedral $[Cu^{I}(TTCN\text{-}\kappa^3)(TTCN\text{-}\kappa^1)]^{2+}$ which then quickly yields tetrahedral **1** with an accompanying conformational change in the TTCN-κ^1 ligand. The principle of microscopic reversibility also requires that tetrahedral **1** may first undergo a geometry change to octahedral **1**, albeit unfavorable, followed by oxidation to octahedral **2** and, similarly, octahedral **2** may first isomerize to tetrahedral **2** followed by reduction as shown in Scheme 1. Although this square mechanism accounted for the originally obtained data, additional studies were warranted to establish the structures proposed for the transient intermediates: tetrahedral **2** and octahedral **1**. The present investigation was undertaken to further study and characterize the proposed short-lived intermediate in the oxidation of **1** to **2** by using time-resolved optical and conductometric measurements with the radiation chemical technique of pulse radiolysis.[15,16] Similar studies of other $[Cu^{I}(TTCN\text{-}\kappa^3)(L)]^+$ complexes, where L is monodentate thiolane (TL), thiane (TN), or 1,4-dithiane (DTN), **5**−**7**, respectively, as well as $[Cu^{I}(18\text{-ane-}S_6)]^+$ (**8**; 18-ane-S_6 = 1,4,7,10,13,16-hexathiacyclooctadecane) also provided insight into this reaction. The structures of all of the ligands and their labels are shown in Figure 1 and the structures of all of the complexes are given in Figure 2. Additional results on the dependence of the electrochemical redox process on pH afforded further evidence on the identity of the transient which correlates with the time-resolved measurements. These new results and NMR spectroscopic studies reveal the oxidation of **1** to **2** to be more complex than previously proposed. In particular, evidence is presented for the importance of ligand dissociation, and **3** is identified as the structure of the Cu(II) intermediate formed en route to octahedral **2**. The essential aspects of this newly adduced mechanism are summarized in Scheme 2, which serves as a guide through the Results and Discussion section for the reader.

Experimental Section

All the experiments were done at ambient temperature (≈20 °C). The solutions were prepared in highly pure deionized (18 MΩ) water. Adjustments of pH were made with $HClO_4$ or NaOH.

Instrumentation and Techniques. All the NMR spectra were acquired on a Bruker AM-500 or Varian XL-300 NMR spectrometer and were referenced to the residual proton impurity in the deuterated solvent. The X-ray crystallographic data were collected according to previously described procedures.[8] Details of the apparatus and procedure for cyclic voltammetry have been described elsewhere.[8] The voltammograms were recorded with a glassy carbon working electrode against a Ag/AgCl (saturated NaCl) reference electrode.

In the pulse radiolysis experiments N_2O-saturated aqueous solutions of the analytes were irradiated with high-energy pulses of electrons to generate •OH radicals. The energy was administered through either 1−2-μs pulses of 1.55-MeV electrons from a van de Graaf accelerator or 50-ns pulses of 15-MeV electrons from a linear accelerator (LINAC). Typically a total energy of 1−3 Gy [1 Gy (Gray) = 1 J kg^{-1}] was released into the system during the pulses. This corresponds to a total •OH radical concentration on the order of 10^{-6} M. The radical concentration was generally smaller than the complex or any other solute concentration. Further details of the pulse radiolysis technique and dosimetry can be found in the literature.[15,16]

Reagents. All the chemicals employed were from Aldrich (Milwaukee, USA) and were used as obtained. $[Cu(TTCN)_2](BF_4)_2$,[11] $[Cu(18\text{-ane-}S_6)]PF_6$,[17] and $[Cu(CH_3CN)_4]PF_6$[18] were synthesized according to the cited literature procedures.

$[Cu(TTCN)(TL)]PF_6$, 5. Exactly the same procedure and quantities of reactants were used for the synthesis of the thiolane (TL) complex as those for the synthesis of the TN complex, described below. The yield was 41%.

Anal. Calcd for $C_{10}H_{20}S_4CuPF_6$: C, 25.18; H, 4.23; S, 26.88; P, 6.49; F, 23.90. Found: C, 25.16; H, 4.16; S, 26.95; P, 6.50; F, 23.71.

$[Cu(TTCN)(TN)]PF_6$, 6. $[Cu(CH_3CN)_4]PF_6$ (410 mg, 1.1 mmol) was added to a solution of TTCN (200 mg, 1.11 mmol) and of thiane (TN) (205 mg, 2 mmol) in methanol (40 mL) which was prepurged with argon. The solution was stirred for about 3 h. The reaction mixture was concentrated on a rotary evaporator until crystallization started and then left overnight at −40 °C. The crystalline product was collected on a sintered glass funnel under argon, washed with diethyl ether, and desiccated. The yield was 56%.

Anal. Calcd for $C_{11}H_{22}S_4CuPF_6$: C, 26.91; H, 4.52; S, 26.12; P, 6.31; F, 23.21. Found: C, 26.81; H, 4.48; S, 26.44; P, 6.52; F, 23.01.

$[(TTCN)Cu(DTN)Cu(TTCN)](PF_6)_2$, 7. To a degassed solution of TTCN (200 mg, 1.11 mmol) and 1,4-dithiane (70 mg, 0.58 mmol) in methanol (25 mL) was added $[Cu(CH_3CN)_4]PF_6$ (410 mg, 1.1 mmol) under stirring. After the solution was stirred for 2 h under Ar, nitromethane (10 mL) was added to dissolve the precipitate. After filtration under Ar the filtrate was concentrated on a rotary evaporator until crystallization started. After overnight refrigeration, the crystalline product was removed by filtration and washed with diethyl ether. The filtrate was then layered carefully with diethyl ether and refrigerated overnight. A second crop of crystals was recovered and processed under Ar. The overall yield was 42%.

Anal. Calcd for $C_{16}H_{32}S_8Cu_2P_2F_{12}$: C, 21.40; H, 3.59; S, 28.56; P, 6.90; F, 25.39. Found: C, 21.32; H, 3.60; S, 28.43; P, 6.83; F, 25.44.

$[Cu(TTCN)(TTCNO)]PF_6$, 9. To a solution of TTCN (1,4,7-trithiacyclononane, 80 mg, 0.443 mmol) and TTCNO[19] (1,4,7-trithiacyclononane 1-oxide, 90 mg, 0.458 mmol) in degassed methanol (30 mL, Fisher, HPLC Grade) was added $[Cu(CH_3CN)_4]PF_6$ (165 mg, 0.443 mmol). The reaction mixture was stirred for 3 h under argon. The

(11) Setzer, W. N.; Ogle, C. A.; Wilson, G. S.; Glass, R. S. *Inorg. Chem.* **1983**, *22*, 266.
(12) Glass, R. S.; Steffen, L. K.; Swanson, D. D.; Wilson, G. S.; de Gelder, R.; de Graaf, R. A. G.; Reedijk, J. *Inorg. Chim. Acta* **1993**, *207*, 241.
(13) Bernardo, M. M.; Schroeder, R. R.; Rorabacher, D. B. *Inorg. Chem.* **1991**, *30*, 1241.
(14) Bernardo, M. M.; Robandt, P. V.; Schroeder, R. R.; Rorabacher, D. B. *J. Am. Chem. Soc.* **1989**, *111*, 1224.
(15) Asmus, K.-D. *Int. J. Radiat. Phys. Chem.* **1972**, *4*, 417.
(16) Asmus, K.-D.; Janata, E. In *The Study of Fast Processes and Transient Species by Electron Pulse Radiolysis*; Baxendale, J. M., Busi, F., Eds.; NATO ASI; D. Reidel: Dordrecht, 1982; pp 91−113.
(17) Hartman, J. R.; Cooper, S. R. *J. Am. Chem. Soc.* **1986**, *108*, 1202.
(18) Kabus, G. J. *Inorg. Synth.* **1979**, *19*, 90.
(19) TTCNO was synthesized following the procedure reported by L. K. Steffen, Ph.D. Thesis, The University of Arizona, 1990.

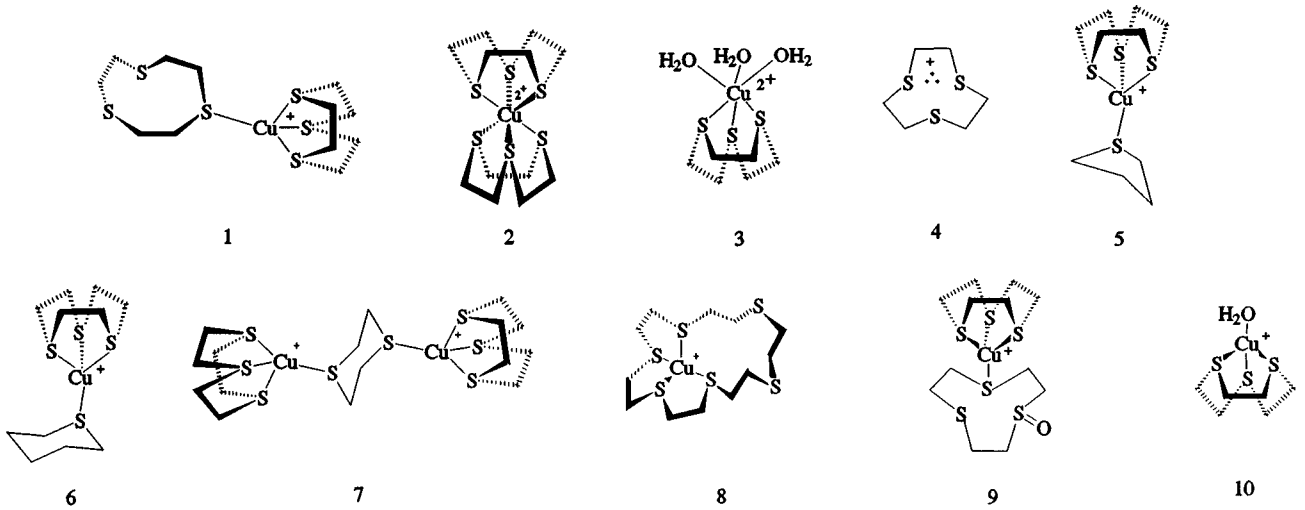

Figure 2. Drawings of the structures of the copper complexes and transients.

Table 1. Crystal Data[a] for $[(TTCN)Cu^{I}(DTN)Cu^{I}(TTCN)](PF_6)_2$ (**7**) and $[Cu^{I}(TTCN)(TTCNO)]PF_6$ (**9**)

	7	**9**
empirical formula	$CuS_4C_8H_{16}PF_6$	$CuS_6C_{12}H_{24}OPF_6$
fw	448.96	
mw	897.92	585.19
space group	*C*2/*c* (No. 15)	$P2_1/n$ (No. 4)
a, Å	19.832(6)	7.939(2)
b, Å	13.396(2)	8.688(3)
c, Å	15.815(4)	15.964(4)
β, deg	133.57(1)	102.94(4)
Z	8	2
crystal color, shape	white, needle	white, prism
R	0.041	0.078
R_w	0.044	0.075
GOF	1.08	1.12

[a] Standard deviation of the least significant figure is given in parentheses.

white powdery product was removed by filtration under argon and washed sequentially with methanol and diethyl ether and dried under vacuum (77% yield): ^{1}H NMR (CD_3CN, 297 K) δ 3.88 (ddd, $2H_a$), 3.36 (ddd, $2H_b$), 3.27 (ddd, $2H_c$), 2.99 (ddd, $2H_d$) [(J_{ab} = 14.3 Hz), (J_{ac} = 2.6 Hz), (J_{ad} = 9.9 Hz), (J_{bc} = 7.4 Hz), (J_{bd} = 2.8 Hz), (J_{cd} = 15.4 Hz)], 2.95 (m, 16 H); ^{13}C NMR (CD_3CN, 297 K) δ 53.5, 35.7, 32.8, 26.2.

Anal. Calcd for $C_{12}H_{24}S_6OCuPF_6$: C, 24.63; H, 4.13; S, 32.87; P, 5.29; F, 19.48. Found: C, 24.48; H, 4.04; S, 32.99; P, 5.22; F, 19.33.

X-ray Single-Crystal Structure Studies. A single crystal of **7** (having approximate dimensions of 0.20 × 0.20 × 0.50 mm) or **9** (having approximate dimensions of 0.20 × 0.30 × 0.40 mm) was mounted on a glass fiber and placed in a Rigaku AFC5R diffractometer. Cu Kα radiation (λ = 1.54178 Å) was used with a graphite monochromator and a 12-kW rotating-anode generator. Cell constants and orientation matrices were obtained from least-squares refinement using the setting angles of a number of carefully centered reflections in an approximate range of 2Θ and are given in Table 1. The monoclinic space group based on the systematic absences at *hkl* for $h + k \neq 2n$ and at *h*0*l* for $l \neq 2n$ was determined to be *C*2/*c* (No. 15) for **7**, and based on the systematic absences at 0*k*0 for $k \neq 2n$ to be $P2_1/n$ (No. 4) for **9**.

The data were collected at a temperature of −160 ± 1 °C for **7** and 23 ± 1 °C for **9**. For **7** ω-scans of several intense reflections, made prior to collection, had an average width of 0.41° at half height with a take-off angle of 6.0°. Scans of (1.57 + 0.30 tan Θ)° were made at a speed of 32.0 deg/min (in ω). Weak reflections ($I < 10.0\sigma(I)$) were rescanned. A total of 2188 reflections were collected for **7** and 1667 reflections for **9**.

The structure was solved by direct methods.[20] The non-hydrogen atoms were refined anisotropically. For **9** the structure refinement was achieved with the bond angle and bond distances restrained to ideal values because the TTCNO ring is disordered. The structures were refined by full-matrix least-squares techniques using neutral-atom scattering factors,[21] and anomalous dispersion terms[22] were included in F_c; the values for $\Delta f'$ and $\Delta f''$ were those of Cromer.[23] All calculations were performed using the TEXSAN[24] crystallographic software package of the Molecular Structure Corporation and the KUDNA crystallographic software package developed at the University of Kansas.[25] The final cycle of full-matrix least-squares refinement was based on 1993 observed reflections ($I > 0.01\sigma(I)$) and 246 variable parameters for **7** and 1389 observed reflections ($I > 0.01\sigma(I)$) and 234 variable parameters for **9**.

Complex **7** has a center of symmetry. The full complex can be obtained by performing the symmetry operation $0.5 - x$, $0.5 - y$, $-z$ on the coordinates of the half complex. Two half PF_6^- counterions are found in the asymmetric unit. A full PF_6^- ion can be obtained by applying the $1 - x$, y, $1.5 - z$ symmetry operation. Several short C−H- - -F contacts are observed which are probably weak hydrogen bonds. Further structural details are given in the Supporting Information.

Binding Constant Determination by NMR Spectroscopy. Titrations of Cu(I) with TTCN monitored by NMR spectroscopy were carried out in acetonitrile as well as in CD_3CN-D_2O mixtures under an Ar atmosphere. Titration of $[Cu(TTCN)_2]PF_6$ with $[Cu(CH_3CN)_4]PF_6$ in CD_3CN-D_2O gave similar results. There were no differences in the chemical shift data in CD_3CN versus CD_3CN-D_2O. The binding constant for the first equivalent of TTCN is extremely high and cannot be determined by NMR spectroscopic methods. The binding constant for the second equivalent of TTCN was calculated[26] using linear and curve fitting equations for the following equilibrium: $[Cu^{I}(TTCN)]^+ + TTCN \rightleftharpoons [Cu^{I}(TTCN)_2]^+$. There was no consistent change in broadening over the titration in the line shape or width.

Results and Discussion

•OH Radical Induced Oxidation. In order to obtain time-resolved information about the possible intermediates in the

(20) Beurskens, P. T. *Technical Report 1984/1*; *Crystallography Laboratory: Toernooieveld*, 6525 *Ed*; Nijmegen: The Netherlands, 1984.
(21) Cromer, D. T.; Waber, J. T. *International Tables for X-ray Crystallography*; The Kynoch Press: Birmingham, England, 1974; Vol. IV, Table 2.2A.
(22) Ibers, J. A.; Hamilton, W. C. *Acta Crystallogr.* **1964**, *17*, 781.
(23) Cromer, D. T. *International Tables for Crystallography*; The Kynoch Press: Birmingham, England, 1974; Vol. IV, Table 2.3.1.
(24) *TEXSAN-TEXRAY Structure Analysis Package*; Molecular Structure Corp.; Woodlands, TX, 1985.
(25) Takusagawa, F. *Crystallographic Computing System*: *KUDNA*; Department of Chemistry, The University of Kansas, 1984.
(26) Connors, K. A. *Binding Constants*; John Wiley: New York, 1987; pp 189−200.

Scheme 1. Originally Proposed Square Mechanism for the Electron-Transfer Reaction of the $[Cu^{II/I}(TTCN)_2]$ System

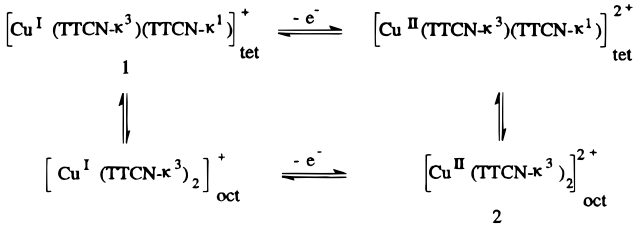

Scheme 2. Reaction Scheme for the Oxidation of **1** to **2**

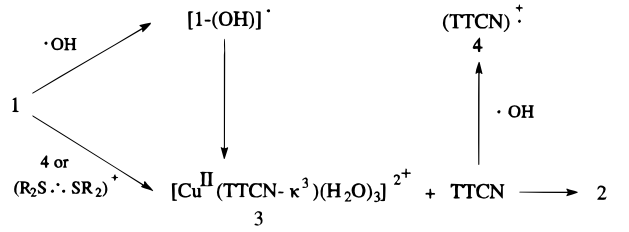

oxidation of **1** to **2** pulse radiolysis experiments were conducted with dilute aqueous solutions of the copper(I) complex and a number of related model compounds. The actual oxidation was achieved by reaction of the complexes with •OH radicals.

The results obtained upon pulse radiolysis of aqueous, N_2O-saturated, 5.0×10^{-5} and 1.0×10^{-4} M solution of **1** at pH 4.0 are displayed in Figures 3 and 4, respectively. The time-resolved spectra and individual absorption traces, recorded on the microsecond to second time scale after a 1-μs pulse, reveal the ultimate formation of a stable product with an absorption peaking at 445 nm (Figures 3b and 4d) whose optical characteristics are identical with those of the well-characterized octahedral complex **2** with both TTCN ligands in the [333] conformation.

The pulse radiolysis experiments further show the formation of two transients in the investigated time interval. The first is a shorter-lived intermediate with λ_{max} at 540 nm, **4**, which converts into a longer-lived species with λ_{max} at 370 nm, **3**, as shown in Scheme 2. This is evidenced by an isosbestic point at 435 nm (Figure 3a) and identical, exponential decay and formation kinetics ($t_{1/2} = 13.7 \pm 0.7$ μs for 10^{-4} M **1**) at the respective maximum wavelengths (Figures 4a and 4b). The 370-nm transient is considerably longer-lived and appears to be the direct precursor of the final and stable oxidation product **2**, as can be deduced from Figure 3b (isosbestic point at 395 nm) and the time-resolved traces in Figures 4c and 4d. The associated kinetics are also described by an exponential rate law with $t_{1/2} = 7.65 \pm 0.30$ ms for 10^{-4} M **1**. The spectra in Figure 3a and the trace displayed in Figure 4b show that a considerable amount of the 370-nm absorption has already developed immediately after the pulse. Since the short-lived 540-nm transient **4** does not exhibit any significant absorption in the 370-nm range (as revealed by other experiments presented later), it is concluded that the 370-nm transient **3** is formed by multiple pathways as shown in Scheme 2. One proceeds through the 540-nm species and, on a much shorter time scale, an •OH adduct of **1**, accounting for about one and two thirds of the 370-nm yield, respectively.

To deduce the structures of the species giving rise to the two transient absorptions various pulse radiolysis experiments were carried out with other oxidizing radicals and with complexes in which the monodentate (TTCN-κ^1) trithia ligand was substituted by heterocycles containing only one sulfur atom.

Change of Oxidant. In order to change the identity of the oxidizing radicals the •OH radical was generated in solutions

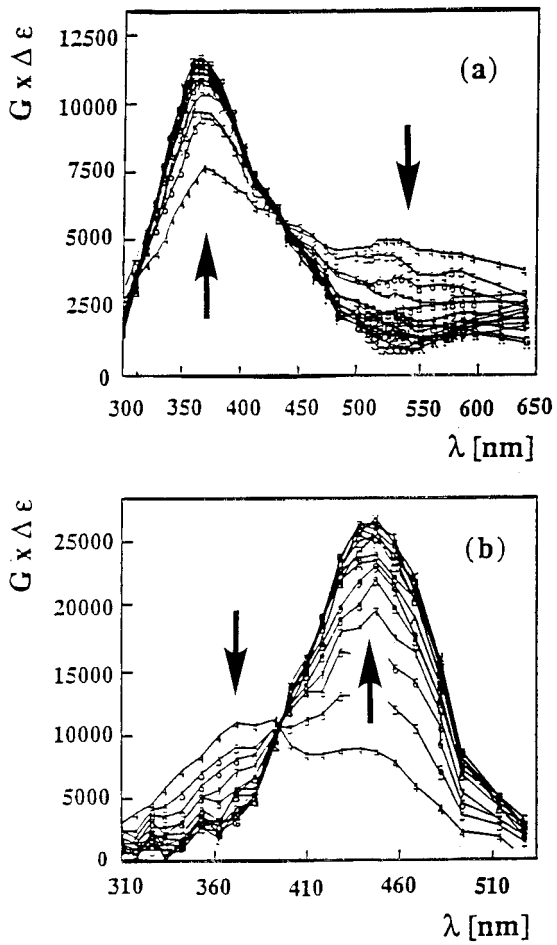

Figure 3. UV/vis spectra of a 5×10^{-5} M, N_2O-saturated aqueous solution of **1** at pH 4 obtained upon pulse irradiation: (a) within 200 μs at steps of 10 μs, and (b) within 100 ms at steps of 5 ms.

containing high concentrations (10^{-3} M) of Me_2S, Et_2S, or free TTCN in addition to that of **1** at $\leq 10^{-4}$ M. In all of these cases the final product **2** (λ_{max} 445 nm) and its immediate precursor, the 370-nm transient, are identical to the •OH-induced oxidation. In each system there is also a precursor of the 370-nm species which, however, shows solute-specific characteristics. For Me_2S and Et_2S these initially formed transients can be identified with the well-known respective $\sigma^2\sigma^{*1}$ three-electron bonded radical cations $(R_2S\therefore SR_2)^+$.[27,28] Under the experimental conditions they are generated within the duration of the 1-μs pulse via the well-established overall reaction shown in eq 1 and exhibit

$$^{\bullet}OH + 2R_2S \rightarrow (R_2S\therefore SR_2)^+ + OH^- \qquad (1)$$

absorption maxima at 465 (R = Me) and 485 nm (R = Et). No 540-nm absorption is observed in these systems.

In the case of solutions containing added TTCN the primary transient exhibits the same absorption features as the 540-nm species in the direct •OH-induced oxidation of **1** except that the total absorption yield at this wavelength is about three times higher. Furthermore, the same absorption with the same high yield is observed in solutions containing only free TTCN and no copper complex. This and the analogy to numerous other examples on the oxidation of polythia compounds[29,30] suggest

(27) Bonifačić, M.; Möckel, H.; Bahnemann, D.; Asmus, K.-D. *J. Chem. Soc., Perkin Trans. 2* **1975**, 675.
(28) Göbl, M.; Bonifačić, M.; Asmus, K.-D. *J. Am. Chem. Soc.* **1984**, *106*, 5984.
(29) Asmus, K.-D.; Bahnemann, D.; Fischer, Ch.-H.; Veltwisch, D. *J. Am. Chem. Soc.* **1979**, *101*, 5322.

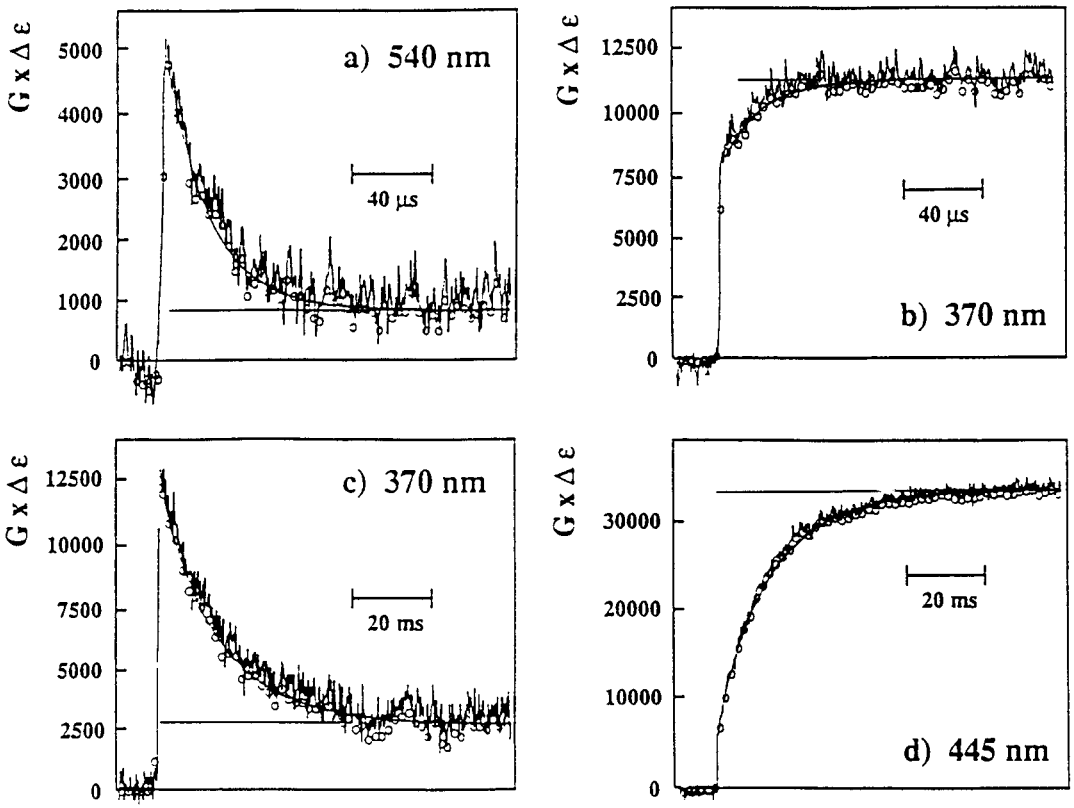

Figure 4. Absorption *vs* time traces at different wavelengths and times of a pulse-irradiated 10^{-4} M, N_2O-saturated aqueous solution of **1** at pH 4: (a) 540 nm (entire time range covered: 200 μs), (b) 370 nm (200 μs), (c) 370 nm (100 ms), and (d) 445 nm (100 ms).

that the 540-nm absorption in the free TTCN containing solutions is due to the $(TTCN)^{\bullet+}$ radical cation **4** formed in the reaction shown in eq 2. The 540-nm absorption in the copper-

$$^{\bullet}OH + TTCN \rightarrow (TTCN)^{\bullet+} + OH^- \qquad (2)$$

(I) complex solution, accordingly, is concluded to result from the oxidation of the TTCN ligand without any direct oxidation of the metal ion. Alternatively, the monodentate TTCN complex may, in fact, dissociate to give $[Cu^{I}(TTCN\text{-}\kappa^3)(H_2O)]^+$, **10**, and TTCN. The free TTCN may then be oxidized to **4**.

Since the longer-lived intermediate **3** absorbing at 370 nm is formed irrespective of the nature of the oxidant, and in all cases with oxidants other than $^{\bullet}OH$, exclusively via one secondary process, its generation is attributed to the following general reaction shown in eq 3. In our specific cases with the added

$$Ox + (\mathbf{1}) \text{ or } (\mathbf{10}) \rightarrow \mathbf{3} \qquad (3)$$

thioethers and free TTCN "Ox" represents $(Me_2S\therefore SMe_2)^+$, $(Et_2S\therefore SEt_2)^+$, or **4**. The fact that **3** is indeed formed via a bimolecular process is proved by the pseudo-first-order kinetics for the decay of the "Ox" and the formation of the 370-nm absorptions. Absolute rate constants derived from the respective concentration dependencies are 2.0 ($\pm$1.0) $\times$ 10^8 M^{-1} s^{-1} for the reaction of both $(R_2S\therefore SR_2)^+$ and 3.5 ($\pm$1.0) $\times$ 10^8 M^{-1} s^{-1} for the reaction of **4** (for a detailed kinetic evaluation of these and other reactions referred to in this paper see ref 31). The underlying reactions involve metal ion oxidation because oxidation of the ligand molecules alone does not yield any comparable absorption in the 370-nm range. Accordingly the oxidation product **3** is a copper(II) complex.

Most interestingly, even in the solutions containing only **1** (no added TTCN) the 540 nm $\rightarrow$ 370 nm conversion is a bimolecular process depending on the copper(I) complex concentration. Moreover, the rate constant of 4.1 ($\pm$1.0) $\times$ 10^8 M^{-1} s^{-1} is practically the same as that for the process in solutions with added TTCN which unambiguously involves free **4**, suggesting that the oxidizing species is, in fact, the same in both cases. This suggests that the oxidized TTCN moiety does not remain attached to the copper ion after oxidation of the complex. Because if it were still bound to the copper, then, in view of the ultimate formation of **2**, an *intra*molecular rather than a bimolecular reaction should have occurred, i.e. $[Cu^{I}(TTCN\text{-}\kappa^3)\{(TTCN\text{-}\kappa^1)^{\bullet+}\}]^{2+} \rightarrow [Cu^{II}(TTCN\text{-}\kappa^3)(TTCN\text{-}\kappa^1)]^{2+}$. The experimental finding, therefore, strongly refutes such a mechanism and indicates detachment of the $(TTCN\text{-}\kappa^1)$ ligand before the 540-nm intermediate can engage in a secondary process. Since Cu(II)$-$S bonds involving thioethers are exceptionally weak, dissociation of the monodentate TTCN ligand is reasonable.

Change of Monodentate Ligand. Further insight into the structure of the transient species is provided by experiments on the $^{\bullet}OH$-induced oxidation of copper(I) complexes in which the monodentate $(TTCN\text{-}\kappa^1)$ ligand was replaced by thiolane (TL), thiane (TN), or 1,4-dithiane (DTN), **5**$-$**7**, respectively (under otherwise identical experimental conditions as for the oxidation of **1**). The structures of the original Cu(I) complexes in which thiolane or thiane replaces the monodentate TTCN ligand are supported by their elemental analyses. The structure of **7**, in which each of the two sulfur atoms of 1,4-dithiane is monocoordinated with each of the two copper ions and thereby bridges them, is established by an X-ray crystallographic study. The crystal data for this complex are given in Table 1, a PLUTO drawing is shown in Figure 5, and complete lists of bond lengths, bond angles, fractional coordinates, and thermal parameters are provided in the Supporting Information. Two results in the $^{\bullet}OH$-induced oxidations of these complexes are particularly noteworthy: (i) in no case is the short-lived 540-nm absorption

(30) Asmus, K.-D. *Acc. Chem. Res.* **1979**, *12*, 436.

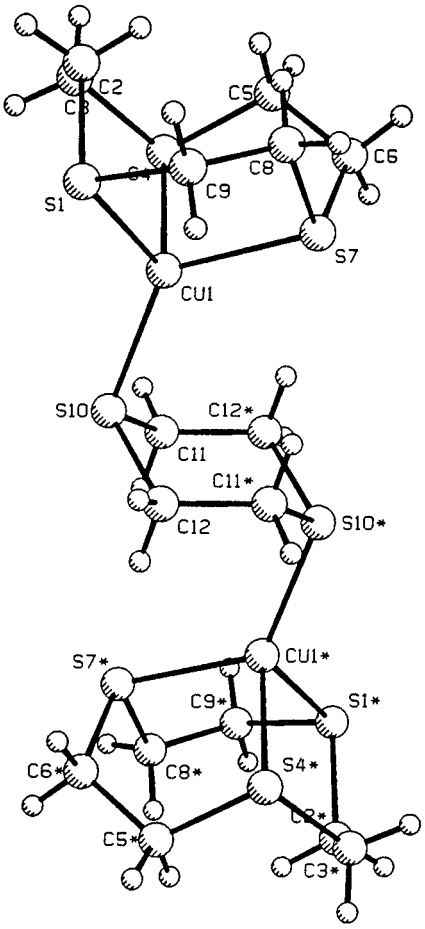

Figure 5. PLUTO drawing of **7**.

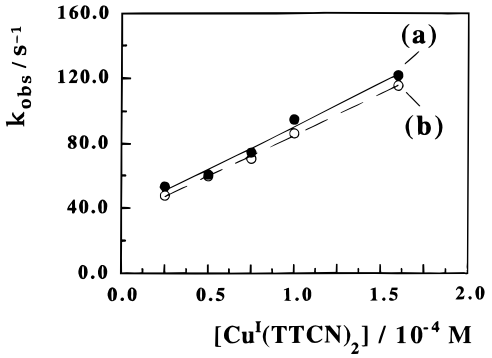

Figure 6. Kinetic analysis of (a) the decay of the transient absorbing at 370 nm and (b) of the formation of **2** at 445 nm in terms of first-order rate constant k_{obs} *vs* [**1**], both at pH 4.

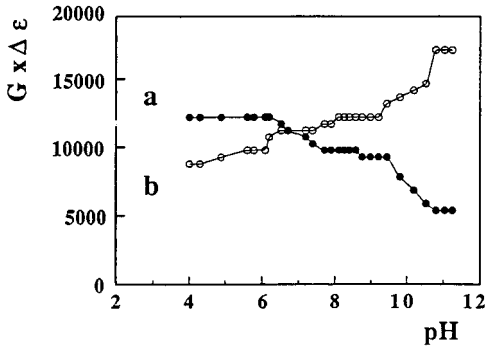

Figure 7. pH dependence of the transient absorptions recorded in a 5 $\times$ 10^{-5} M, N_2O-saturated aqueous solution of **1** 200 μs after the pulse: (a) at 380 nm and (b) at 340 nm.

observed, and (ii) in all cases, however, **3** is formed and eventually converted into the octahedral **2**. The first finding corroborates our conclusion that the 540-nm species results from oxidation of the monodentate or free TTCN ligand. The second finding demonstrates that the nature of the monodentate ligand is irrelevant for the optical properties of **3**. This could, in principle, be explained by a complete lack of electronic contribution from the monodentate ligand to the relevant optical transition. However, a more likely explanation is that the same transient **3** is produced in all cases. This can result by detachment of the monodentate ligand from the central copper ion in the oxidation process, or prior to it. In the case of oxidation of **1** either the oxidized (TTCN-κ^1) (as suggested based on the kinetic results above) or the unoxidized (TTCN-κ^1) may detach.

Dependence of the Formation of 2 on the Concentration of 1. Further support for dissociation of a TTCN ligand can be derived from the kinetics for the conversion of **3** into the final, stable complex **2**. In the "square mechanism" an assumed tetrahedral $[Cu^{II}(TTCN\text{-}\kappa^3)(TTCN\text{-}\kappa^1]^{2+}$ intermediate with both TTCN rings still attached to Cu(II) would only have to undergo a conformational change to form the stable product and this should be a true first-order process. Under the conditions of the pulse radiolysis experiments, however, the decay of the absorption at 370 nm and the corresponding formation at 445 nm is only of pseudo first order and linearly depends on the concentration of the unoxidized copper(I) complex as shown in the plot of the measured first order rate constant as a function of the concentration of **1** in Figure 6. At concentrations $\geq 10^{-4}$ M the bimolecular process is clearly dominating and any true first-order contribution, potentially associable with the intercept, becomes of lesser importance. Formation of **2** thus requires **3** to react with an unoxidized copper(I) complex, and/or the free TTCN which is liberated in the possible dissociation equilibrium with it.

The bimolecular rate constant for this process, calculated from the slope of the straight line in Figure 6, is 5.2 ($\pm$0.5) $\times$ 10^5 M^{-1} s^{-1}. This low value indicates relatively high energetic and/or entropic demands for the formation of **2**. That such a bimolecular process, nevertheless, prevails over a presumably much faster *intra*molecular conformational rearrangement strongly suggests that the latter is, in fact, not possible simply because the second TTCN ligand is not present in **3**.

Alternatively, the TTCN ligand required for the transformation of **3** into **2** can be supplied by purposely added free, uncomplexed TTCN. In this case, the rate constant for the conversion of **3** into **2** becomes somewhat larger. It is found to be 8.4 ($\pm$0.8) $\times$ 10^5 M^{-1} s^{-1}.

pH Dependence. Another relevant observation is that the optical absorption spectrum of **3** varies with pH. The spectrum displayed in Figure 3a with λ_{max} 370 nm shows these optical characteristics only at pH $\leq$6, and the maximum is gradually shifted to lower wavelengths with increasing pH. At pH 10.1, for example, it peaks at 345 nm. The entire pH dependence, recorded at 380 and 340 nm, respectively, is plotted in Figure 7. It shows two practically complementary curves with a clear indication for one breakpoint at pH $\approx$10, and at least one other, possibly even two, in the pH 5$-$7 range. Since it is reasonable to assign such breakpoints to pK_a values, the question is at which sites the protonations occur. Because the thioether sulfur is not sufficiently basic, particularly if attached to the positive copper ion, the sites of protonation must be copper-coordinated OH moieties.

Such sites can be formed most simply by association of an $^{\bullet}$OH radical with the copper(I) and subsequent electron transfer followed by the introduction of an oxo ligand into the coordina-

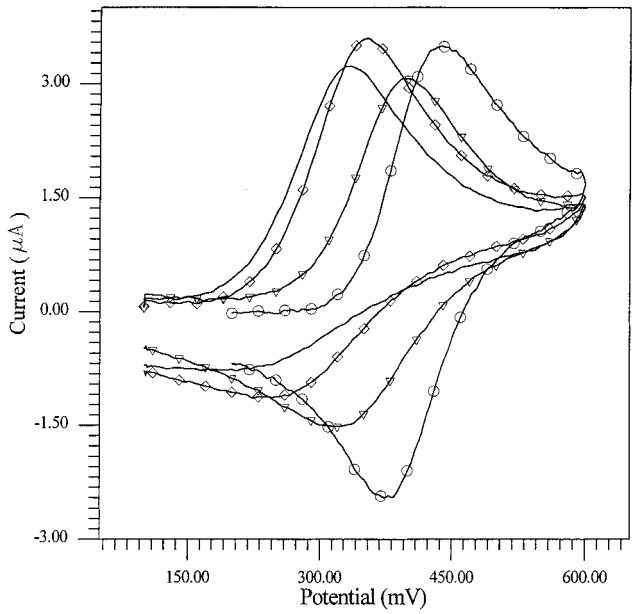

Figure 8. Variation of the cyclic voltammograms of **1** with pH (0.1 M $NaBF_4$, glassy carbon electrode *vs* Ag/AgCl, saturated NaCl): (○) pH3; (△) pH 6; (□) pH 7; (—) pH 8.5.

tion sphere of Cu(II), as shown in eq 4.

$$^{\bullet}OH + \mathbf{1} \rightarrow [Cu^{I}(TTCN\text{-}\kappa^3)(TTCN\text{-}\kappa^1)]^{+}(^{\bullet}OH) \rightarrow [Cu^{II}(OH^{-})(TTCN\text{-}\kappa^3)(TTCN\text{-}\kappa^1)]^{+} \quad (4)$$

However, to account for the apparent further pK_a values additional protonation sites must be introduced. Indeed, dissociation of the monodentate TTCN ligand and coordination of a total of three OH^- groups provides octahedral Cu(II) with three pK_a values expected in the range observed. Furthermore, this proposal for dissociation of the monodentate TTCN ligand is consistent with the kinetic results described above. (See the section on conductivity as well.)

Note also that with increasing pH the rate constant for the formation of **2** decreases. At pH 7, for example, it has dropped by one order of magnitude to $\approx 7 \times 10^4$ M^{-1} s^{-1} as compared to that of 5.2×10^5 M^{-1} s^{-1} at pH ≤ 5. Above pH 8, in fact, less and less of the stable **2** is formed and another process appears to take over, in which the transient decays independent of the copper(I) complex concentration, and a different, non-absorbing product is formed. (The latter process may involve hydrolysis, but no product assignment is possible at present.)[31]

The redox chemistry of **1** at a solid electrode also varied substantially with increasing pH. Figure 8 shows a number of voltammograms of this complex run under different pH conditions. The shift in the formal potential toward less positive values with increasing pH with a large break in the potential−pH curve at pH 6.5 indicates the involvement of an acid−base reaction in the electron-transfer mechanism of the complex. Also the incremental suppression and finally the disappearance of the reverse (cathodic) peak with increasing pH suggest that successive formation of Cu(II) hydroxo complexes makes their subsequent displacement by free TTCN increasingly more difficult. When the cyclic voltammograms of **1** were run in the presence of free TTCN at pH 3, both the anodic and cathodic peaks shifted to a less positive potential by about 10 mV with an apparent increase in the slope of the peaks. Thus the dependence of the electrochemistry of this complex on both the pH and the concentration of TTCN is consistent with

(31) Hungerbühler, H.; Guldi, D.; Asmus, K.-D.; Sanaullah; Schöneich, C.; Wilson, G. S.; Glass, R. S. To be submitted for publication.

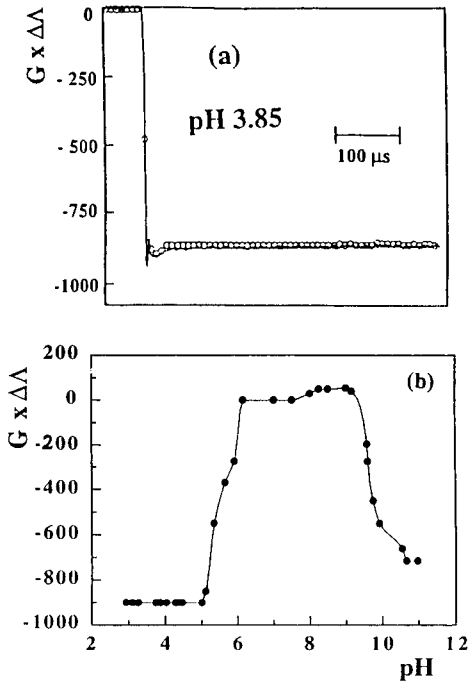

Figure 9. Conductivity *vs* time trace at pH 3.85 (a) and pH dependence of maximum yield of conductivity changes (b), obtained upon pulse irradiation of a 5×10^{-5} M, N_2O-saturated aqueous solution of **1**.

dissociation of the monodentate TTCN ligand and acidic water ligands coordinated to Cu(II). The similar characteristics of the electrochemical metastable species generated by oxidation of **1** and the transient precursor of **2** formed by pulse radiolysis of this complex argue that these are the same species.

Conductivity Experiments. The suggestion that hydroxyl ligands are involved in the UV intermediate and possibly even replace the monodentate (TTCN-κ^1) is further supported by time-resolved conductivity experiments. Figure 9a shows, as an example, the respective trace recorded from a pulsed, pH 3.85, N_2O-saturated solution of 5×10^{-5} M **1**. The negative signal developing after the pulse is indicative of a conductivity loss. With time it attains a constant value[32] of $G \times \Delta\Lambda = -900$ S cm^2. With increasing copper(I) complex concentration the conductivity loss, and consequently the yield, further increases a bit but eventually levels off at $G \times \Delta\Lambda = -1200$ S cm^2 at $\geq 2 \times 10^{-4}$ M. To interpret these results it is important to note that neither the conversion of **4** to **3** nor the conversion of the latter to the final complex **2** is accompanied by any conductivity change. Furthermore, as can be seen from Figure 9b, the change in the loss of conductivity becomes smaller at pH >5, with practically no change between pH 6 and 9, and becomes negative again at pH >9 with a leveling-off value of $G \times \Delta\Lambda = -700$ S cm^2 at pH ≥ 10.5. For the high pH range the overall negative change is attained by a process which starts from a small positive value, present immediately after the pulse ($G \times \Delta\Lambda = 150-300$ S cm^2), and then parallels the **4** → **3** conversion, quite in contrast to the conductivity kinetics on the acid side.

Qualitatively, the conductivity data obtained on the acid side would be compatible with the original suggestion that a tetrahedral $[Cu^{II}(TTCN\text{-}\kappa^3)(TTCN\text{-}\kappa^1)]^{2+}$ transient is formed on oxidation of the Cu(I) complex. In this case, the initial conductivity changes would be accounted for by the following hypothetical reactions referring to oxidation of either the copper or the (TTCN-κ^1) ligand in **1** as shown in eqs 5 and 6, or the

(32) G represents yield in terms of the number of the species formed per 100 eV of absorbed energy. $G = 1.0$ corresponds to 0.1036 μM species produced per joule of absorbed energy. $\Delta\Lambda$ is the change in conductivity in Siemens (S).

copper in **10** as shown in eq 7.

$$^{\bullet}OH + \mathbf{1} \rightarrow [Cu^{II}(TTCN\text{-}\kappa^3)(TTCN\text{-}\kappa^1)]^{2+} + OH^- \quad (5)$$

$$^{\bullet}OH + \mathbf{1} \rightarrow [Cu^{I}(TTCN\text{-}\kappa^3)(TTCN\text{-}\kappa^1)^{\bullet+}]^{2+} + OH^- \quad (6)$$

$$^{\bullet}OH + \mathbf{10} \rightarrow [Cu^{II}(TTCN\text{-}\kappa^3)(H_2O)]^{2+} + OH^- \quad (7)$$

In the acid environment all of these reactions would be followed by immediate neutralization of the hydroxide ion as shown in eq 8. The overall net result in either case would be the

$$OH^- + H_{aq}{}^+ \rightarrow H_2O \quad (8)$$

replacement of one "normal" cationic charge ($\Lambda = 45$ S cm^2 at 18 °C) at the expense of a highly conducting $H_{aq}{}^+$ ($\Lambda = 315$ S cm^2 at 18 °C), i.e., $\Delta\Lambda = -270$ S cm^2. Since a conversion of $[Cu^{I}(TTCN\text{-}\kappa^3)(\{TTCN\text{-}\kappa^1\}^{\bullet+})]^{2+}$ into $[Cu^{II}(TTCN\text{-}\kappa^3)(TTCN\text{-}\kappa^1)]^{2+}$ would not lead to any significant conductivity changes, the combined yield of the two initial reactions would equal the yield of $^{\bullet}OH$ radicals, namely, $G(^{\bullet}OH) = 6$. The actual yield, calculated from the conductivity measurements, amounts, however, only to $G = 4.45$ with an error limit of no more than ± 0.5. This discrepancy alone would not pose a serious problem, however, because some of the hydroxyl radicals could abstract a hydrogen atom from the TTCN moieties, a reaction not involving changes in conductivity and well known for thioether oxidations.[27] However, the above scheme is incompatible with the conductivity results in basic solutions where, in contrast to the experimental result, all the potential OH^- releasing reactions (eqs 5−7) would call for an increase in conductivity because the hydroxide ion would not be neutralized anymore. In essence, like all the other pulse radiolysis experiments the conductivity experiments also require a structure for **3** which is different from a simple tetrahedral $[Cu^{II}(TTCN\text{-}\kappa^3)(TTCN\text{-}\kappa^1)]$.

Identity of 3, the Precursor of 2. A structure of **3** compatible with all of the experimental data and conclusions is that shown in Figure 2. Its formation is suggested to arise via an initial $^{\bullet}OH$ radical addition to the Cu(I) complex in the overall reaction shown in eq 9. To identify a possible $^{\bullet}OH$ adduct pulse

$$\mathbf{1} + {}^{\bullet}OH \rightarrow [Cu^{I}(TTCN\text{-}\kappa^3)(TTCN\text{-}\kappa^1)]^{+}({}^{\bullet}OH) \xrightarrow[2H_2O]{H^+} [Cu^{II}(TTCN\text{-}\kappa^3)(H_2O)_3]^{2+} + TTCN \quad (9)$$
$$\mathbf{3}$$

radiolysis was extended into the nanosecond time scale. Indeed, a very short-lived absorption with λ_{max} at 260 nm was observed which decays by a true first-order process ($k = 1.4 \times 10^6$ s^{-1}) directly into **3** and accounts for the fast-formed portion on the microsecond time scale experiment in Figure 4b. (As will be discussed in detail elsewhere[31] this absorption is likely to be due to an $^{\bullet}OH$ adduct to any one of the copper-bound sulfur atoms in the TTCN ligand rather than a hydroxyl adduct to the copper ion.)

The second, slower process of the formation of **3** in Figure 4b is accordingly assignable to an oxidation of the copper(I) complex by **4** (irrespective of whether this is detached from the metal or not), followed or accompanied by a fast TTCN ↔ OH^- ligand exchange and coordination of water, as shown in eqs 10 and 11. [The $[Cu^{I}(TTCN\text{-}\kappa^3)]$ complex fragment is likely to coordinate a water molecule as fourth ligand[33] unless it encounters a free TTCN in which case an original copper(I) complex is regenerated.] As formulated, both overall mechanisms, i.e., via the $^{\bullet}OH$ adduct or TTCN oxidation, are in accord with the conductivity data observed in the acidic solution. To accommodate the data in the neutral and basic pH range consecutive deprotonation is inferred as formulated in eqs 12−14.[34]

$$^{\bullet}OH + \mathbf{1} \rightarrow OH^- + (TTCN\text{-}\kappa^1)^{\bullet+}_{\text{free/complexed}} + [Cu^{I}(TTCN\text{-}\kappa^3)] \quad (10)$$

$$(TTCN\text{-}\kappa^1)^{\bullet+}_{\text{free/complexed}} + \mathbf{1} + H^+ + 2H_2O \rightarrow \mathbf{3} + 2TTCN \quad (11)$$

$$[Cu^{II}(TTCN\text{-}\kappa^3)(H_2O)_3]^{2+} \rightleftharpoons [Cu^{II}(TTCN\text{-}\kappa^3)(OH^-)(H_2O)_2]^{+} + H_{aq}{}^+ \quad (12)$$

$$[Cu^{II}(TTCN\text{-}\kappa^3)(OH^-)(H_2O)_2]^{+} \rightleftharpoons [Cu^{II}(TTCN\text{-}\kappa^3)(OH^-)_2(H_2O)] + H_{aq}{}^+ \quad (13)$$

$$[Cu^{II}(TTCN\text{-}\kappa^3)(OH^-)_2(H_2O)] \rightleftharpoons [Cu^{II}(TTCN\text{-}\kappa^3)(OH^-)_3]^{-} + H_{aq}{}^+ \quad (14)$$

From the conductivity point of view the absence or presence of H_2O ligands is, of course, irrelevant and, in principle, a second TTCN could also still be attached. In order to account for the observed conductivity signals in basic solutions at higher pH it is, however, necessary to invoke a total of three OH^- ligands. The proposed structure of **3** with its three acid−base forms is, therefore, the most reasonable possibility because it is the simplest one which fits the data.

This conclusion is also consistent with a number of non-pulse-radiolysis observations described below and in the following sections. It involves hydrolysis of the monodentate $(TTCN\text{-}\kappa^1)$ in the unoxidized copper(I) complex as shown in eq 15.

$$\mathbf{1} + OH^- \rightleftharpoons [Cu^{I}(TTCN\text{-}\kappa^3)(OH^-)] + TTCN \quad (15)$$

This is compatible with the instability of **1** in basic solution, and with titration experiments which indicate a p$K \approx 6.5$ (± 0.2) for this equilibrium. Assuming that $[Cu^{I}(TTCN\text{-}\kappa^3)(OH^-)]$ is the prevalent form at the high pH range of our experiments, i.e. at pH ≥ 10.5, and the reaction of the $^{\bullet}OH$ radical with $[Cu^{I}(TTCN\text{-}\kappa^3)(OH^-)]$ and free TTCN (which under these circumstances are present at equal concentration) occur with the same rate constant, the yield of both reaction routes would be equal, i.e. occur each with $G \approx 3$. Quantitatively, this translates into the following experimental data to be expected at high pH (for detailed calculations see ref 31): (i) Oxidation of the $(TTCN\text{-}\kappa^1)$ ligand, to yield **4**, results in a conductivity increase of $G\times\Delta\Lambda \approx +700$ S cm^2 and oxidation of $[Cu^{I}(TTCN\text{-}\kappa^3)(OH^-)]$, to yield $[Cu^{II}(TTCN\text{-}\kappa^3)(OH^-)_3]^-$, leads to a loss of $G\times\Delta\Lambda \approx -500$ S cm^2. Since both processes occur fast the combined signal observable immediately after the pulse amounts to $G\times\Delta\Lambda \approx +200$ S cm^2. (ii) The secondary oxidation of $[Cu^{I}(TTCN\text{-}\kappa^3)(OH^-)]$ by **4** involves a loss of $G\times\Delta\Lambda \approx -1100$ S cm^2, and the overall signal should thus attain a final value of $G\times\Delta\Lambda \approx -900$ S cm^2 with kinetics entirely controlled by this secondary process. Considering the various possible uncertainties involved (yield and specific conductances) this proposed scheme is in excellent agreement with the experimental results.

(33) Olmstead, M. M.; Musker, W. K.; Kessler, R. M. *Transition Met. Chem.* **1982**, *7*, 140.

(34) Copper complexes are also known to form μ-oxo species under basic conditions. However, these are omitted from consideration for simplicity because they would not affect the conclusions drawn from the experiments described in this paper.

The three equilibria (eqs 12−14) also provide an excellent basis to explain the observed optical changes. In fact, the blue-shift with increasing (H_2O) → (OH^-) ligand conversion probably makes good sense from the electronic point of view. Finally, both our optical and conductivity data allow the extraction of at least two of the equilibrium constants with a reasonable degree of confidence, namely, p$K_a \approx 5.6$ (±0.3) for this first and ≈9.7 (±0.5) for the third equilibrium. The value for the second is more difficult to evaluate, but it should be close to that of the hydrolysis of **1**, i.e., ≈7 to account for the overall near zero conductivity change in the pH ≤9 range.

Compatibility with the Formation Kinetics of 2. The equilibria formulated in eqs 12−14 also afford a satisfactory explanation for the pH dependence of the conversion kinetics of the copper(II) transient into the final, stable complex **2**. Since the transient contains only one TTCN ligand it needs to acquire the second one from outside in a bimolecular process. In acid solutions the source of this ligand is unoxidized **1** and/or possibly free TTCN. The corresponding reaction with **1**, shown in eq 16, is envisaged to proceed via an initial interaction of

$$[Cu^{II}(TTCN\text{-}\kappa^3)(H_2O)_3] + \mathbf{1} \rightarrow \mathbf{2} + \text{other products} \quad (16)$$

the copper(II) intermediate with the two free sulfurs in the monodentate (TTCN-κ^1) of the copper(I) complex.[8] Associated with this first step is a displacement of two water ligands. This is then followed by the complete detachment of the (TTCN-κ^1) ligand from the Cu(I) ion, possible structural change to an all-endodentate [333] conformation, and ultimate displacement of the third water ligand in the Cu(II)species. The complexity of the overall process provides a most reasonable rationale for high steric demands and/or activation energy, and thus for the relatively low rate constant. The fact that the reaction of the copper(II) intermediate with added free TTCN occurs only marginally faster (8.4×10^5 M^{-1} s^{-1} *vs* 5.2×10^5 M^{-1} s^{-1}) would indicate that the detachment of the monodentate ligand and the possibly necessary adoption of the [333] conformation of the incoming TTCN are energetically of less importance than the actual ligand exchange process in the copper(II) complex. This conclusion is also supported by the NMR spectroscopic data presented below.

The proposed identity of the copper(II) transient not only explains the independence of its properties from the nature of the monodentate ligand in the unoxidized copper(I) complex, it equally well explains the much slower conversion of the transient into the final complex **2** for all [Cu^I(TTCN-κ^3)(L)] systems with L ≠ TTCN because in these systems the only TTCN available is a relatively tightly bound (TTCN-κ^3). Of course, when free TTCN is added the rate of reaction becomes correspondingly faster and attains, as expected, a common value for all systems.

The suggested structure of the copper(II) transient also provides a plausible rationale for the pH dependence of the formation of **2**. Thus the fastest reaction occurs at pH ≤5 when the incoming TTCN has to replace three water ligands. At higher pH the rate decreases practically parallel to the successive conversion of these water ligands into hydroxide ligands which, because of their negative charge, are more strongly bound to the positive Cu^{2+} ion and consequently require higher activation energy to be replaced. Eventually two, and finally all three, water ligands will be hydroxides and their replacement by (TTCN-κ^3) becomes, in fact, too slow to compete with other decay routes of the transient.

The overall low bimolecular rate constant for the incorporation of the second TTCN ligand also makes sense in view of Cu^{2+} being a hard acid, preferring the hard oxo ligands over the softer sulfur. In fact, it seems to need the entire entropic advantage of chelation of a tridentate TTCN ligand to stabilize the structure of **2**. How sensitive this system responds even to the subtle differences in the complex geometry emerges from an experiment with [Cu^I(18-ane-S_6)]$^+$, **8**. The cyclic 18-ane-S_6 ligand contains six sulfur atoms, each two of them separated by a $-(CH_2)_2-$ unit as in TTCN. In the copper(I) complex four of the sulfurs are coordinated with the copper, satisfying the tetrahedral preference of Cu(I), while the remaining two are not. This complex could be an ideal system for a fast and *intra*molecular hexacoordination once the copper is oxidized. Indeed, in the •OH-induced oxidation there is no indication of a long-lived intermediate absorbing at 370 nm, and only a fast (within ≈5 μs) formation of an absorption around 450 nm, seemingly characteristic for hexasulfur-coordination, is observed. What is interesting, however, is the limited lifetime of this product. Even in acid solution it decays with $t_{1/2} \approx 7$ ms. (In basic solution the decay is further accelerated, e.g., $t_{1/2} \approx 750$ μs at pH 8.3.) This finding suggests that the coordination geometry of **2** cannot be achieved by **8**. The initial fast formation of a hexasulfur-coordinate intermediate in the oxidation of **8** is expected because the additional two sulfur atoms ligated after the copper oxidation would be the two originally non-coordinated sulfurs in 18-ane-S_6. However, the geometry attainable in this complex apparently does not afford the thermodynamically most favorable structure. It is conceivable, and in agreement with crystal structure analysis,[17] that **2** does not adopt octahedral CuS_6 coordination geometry of highest symmetry but involves two different sulfur−sulfur distances, one within and another between the respective [333] units. In 18-ane-S_6 ligand all sulfurs are equally spaced by two methylene groups and in order to attain the apparently most favorable **2** structure the two linking $-S-(CH_2)_2-S-$ units need to be constrained, and this would make at least one (or possibly even more) sulfur(s) susceptible for eventual replacement by oxo ligands. Similarly in the oxidation of [Cu^I(15-ane-S_5)]$^+$, in which the metal ion coordinates only four sulfur atoms of the ligand, coordination of the fifth sulfur atom becomes extremely rapid once the Cu^I is oxidized to Cu^{II}.[35] Nevertheless, this additional Cu−S bond is suggested[35] to be weak.

Ligand Dynamics in 1. The pulse radiolysis experiments show that **1** on oxidation undergoes loss of the monodentate TTCN ligand or that the monodentate TTCN ligand dissociates and it is **10** which is oxidized.

NMR spectroscopic studies provide some insight into the ligand dynamics in **1** that are not redox coupled. The ^{1}H NMR spectrum of TTCN shows a singlet at δ 3.08 ppm. Thus all of the hydrogen atoms in this molecule are equivalent. Assuming that the lowest energy conformer in solution for TTCN is [333],[9,36,37] the equivalency of the hydrogen atoms is accommodated by rapid interconversion of the gauche conformers as suggested by Lockhart and Tomkinson,[38] and ring inversion of the endodentate [333] conformers on the NMR time scale. Titration of TTCN with Cu(I) in a 1:1 mixture of CD_3CN/D_2O monitored by ^{1}H NMR spectroscopy gave the results shown in Figure 10. As Cu(I) is added the signal broadens and undergoes an upfield shift. At a 1:1 ratio of Cu(I) to TTCN two broad peaks are observed and beginning with a 3:2 and continuing with higher ratios of Cu(I) to TTCN an unchanging AA′BB′

(35) Vande Linde, A. M. Q.; Juntunen, K. L.; Mols, O.; Ksebati, M. B.; Ochrymowycz, L. A.; Rorabacher, D. B. *Inorg. Chem.* **1991**, *30*, 5037.
(36) Setzer, W. N.; Coleman, B. R.; Wilson, G. S.; Glass, R. S. *Tetrahedron* **1981**, *37*, 2743.
(37) Blom, R.; Rankin, D. W. H.; Robertson, H. E.; Schröder, M.; Taylor, A. *J. Chem. Soc., Perkin Trans. 2* **1991**, 773.
(38) Lockhart, J. C.; Tomkinson, N. P. *J. Chem. Soc., Perkin Trans. 2* **1992**, 533.

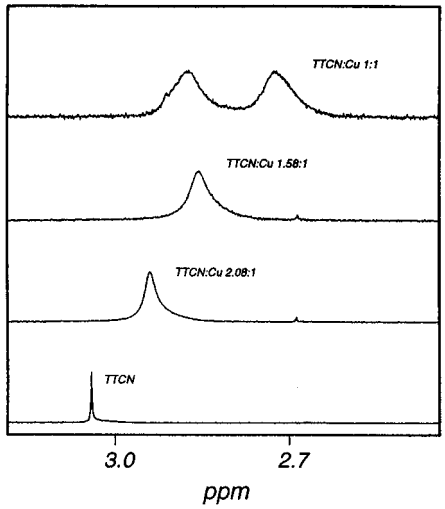

Figure 10. Titration of TTCN with Cu(I) in CD_3CN/D_2O monitored by ^1H NMR spectroscopy.

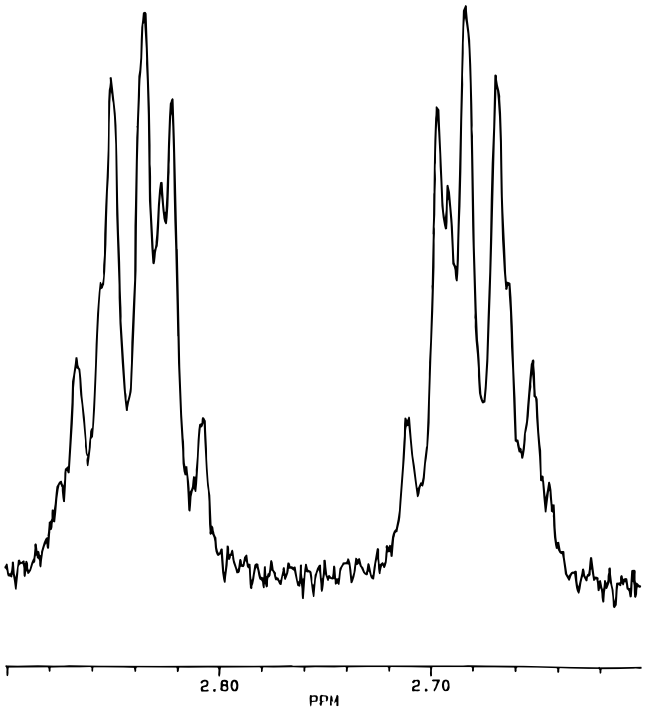

Figure 11. ^1H NMR spectrum of a CD_3CN/D_2O solution containing a 3:2 ratio of Cu(I):TTCN.

pattern is obtained as exemplified by Figure 11. Under these conditions there is apparently no free TTCN in solution and the tridentate TTCN ligand gives rise to the observed spectrum. This suggests that the first TTCN molecule coordinated to Cu(I) binds strongly as a tridentate ligand but that the second TTCN ligand bound to $[Cu^I(TTCN\text{-}\kappa^3)]$ exchanges with unbound TTCN. In addition the spectrum shown in Figure 11 suggests that coordination of TTCN to Cu(I) as a tridentate ligand prevents ring inversion but not interconversion of the two gauche forms. In addition, under these conditions when the ratio of Cu(I) to TTCN is 2:3, there is still no free TTCN because stoichiometry requires that the additional TTCN be bound to $[Cu^I(TTCN\text{-}\kappa^3)]^+$. This additional TTCN is monodentate owing to the preferential four-coordination of Cu(I) as shown in the X-ray crystallographic structure of $[Cu^I(TTCN)_2]PF_6$.[8] However, at room temperature the ^1H NMR spectrum shows equivalent TTCN ligands. Consequently, the tridentate and monodentate TTCN ligands must interconvert rapidly on the NMR time scale. More insight into this process was obtained

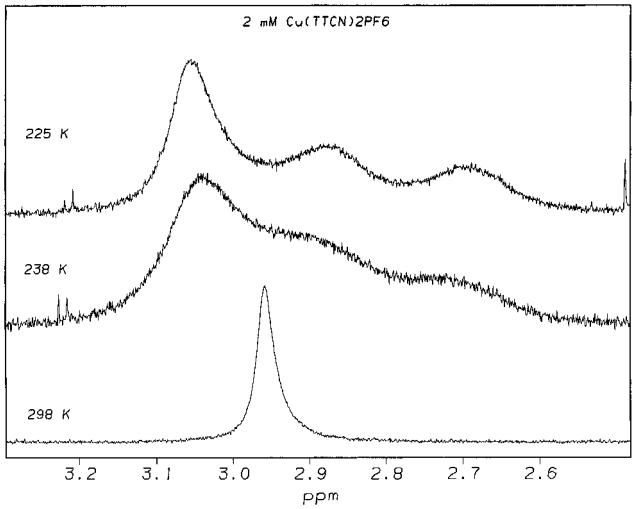

Figure 12. ^1H NMR spectra of $[Cu(TTCN)_2]PF_6$ in CD_3CN at various temperatures.

by variable-temperature NMR spectroscopic studies on $[Cu^I(TTCN)_2]^+$ in CD_3CN. As shown in Figure 12, as the temperature is lowered the peak broadens and then separates into three resonances. Below 225 K the solution freezes but at this temperature the ratio of the three peaks determined by integration is 2:1:1. This suggests that the interconversion of tridentate and monodentate TTCN ligands has been frozen out. The monodentate TTCN absorbs at $\delta \sim 3.05$ with its twelve magnetically equivalent protons and at $\delta \sim 2.86$ and ~ 2.68 by the tridentate TTCN with its marginally resolved axial and equatorial protons, respectively. The equivalence of the protons of monodentate TTCN suggests that not only is this ligand conformationally mobile but that each of the sulfur atoms may be bonded to the Cu^I, i.e., there are metallotropic shifts.[39,40] Such fluxional behavior is analogous to that suggested for $[Pd(TTCN)_2](BF_4)_2$ which shows a singlet in its ^1H NMR spectrum even at 238 K but its solid state structure shows a square plane of four sulfur donors and two weak apical interactions.[41] Thus metallotropy is suggested in this case to account for the NMR spectroscopic equivalence of the ligand hydrogen atoms.

To reduce metallotropy in the monodentate TTCN and interchange of the monodentate and tridentate TTCN ligands, the $[Cu^I(TTCN\text{-}\kappa^3)(TTCNO\text{-}\kappa^1)]^+$ complex **9**, in which the monodentate ring is the mono-*S*-oxide of TTCN, was prepared and studied. The desired mixed ligand complex selectively crystallized from a 1:1:1 molar mixture of TTCN, TTCNO, and $[Cu^I(CH_3CN)_4]PF_6$. Its structure was determined by X-ray crystallographic methods. The crystal data for this complex are given in Table 1, a PLUTO drawing of this complex is given in Figure 13, and complete lists of bond lengths, bond angles, fractional coordinates, and thermal parameters are provided in the Supporting Information. The CuS_4 coordination geometry is tetrahedral with three sulfur atoms from one TTCN coordinated in the endodentate [333] conformation and, in the fourth coordination site, with one of the thioether not sulfoxide-sulfur atoms in the monodentate TTCNO ring. This complex undergoes irreversible oxidation at a peak potential more positive than that for $[Cu^I(TTCN\text{-}\kappa^3)(TTCN\text{-}\kappa^1)]^+$ as shown in Figure 14a. It will be noted that the reduction of the Cu(II) complex resulting from oxidation of **9** occurs at exactly the same potential

(39) Abel, E. W.; Beer, P. D.; Moss, I.; Orrell, K. G.; Sik, V.; Bates, P. A.; Hursthouse, M. B. *J. Organomet. Chem.* **1988**, *341*, 559.
(40) Bernardo, M. M.; Heeg, M. J.; Schroder, R. R.; Ochrymowycz, L. A.; Rorabacher, D. B. *Inorg. Chem.* **1992**, *31*, 191.
(41) Blake, A. J.; Holder, A. J.; Hyde, T. I.; Roberts, Y. V.; Lavery, A. J.; Schröder, M. *J. Organomet. Chem.* **1987**, *323*, 261.

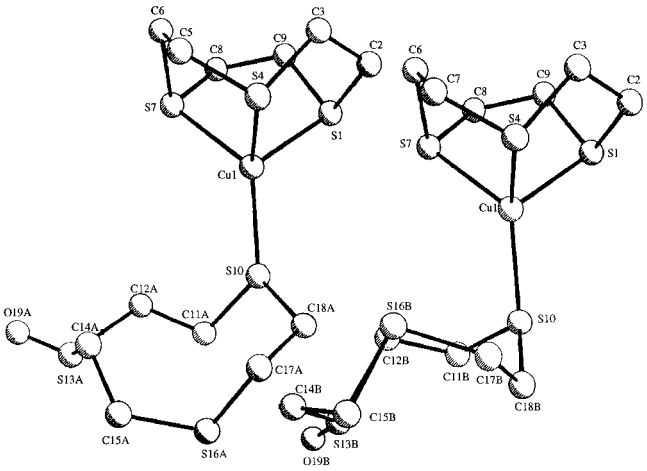

Figure 13. PLUTO drawing of **9**.

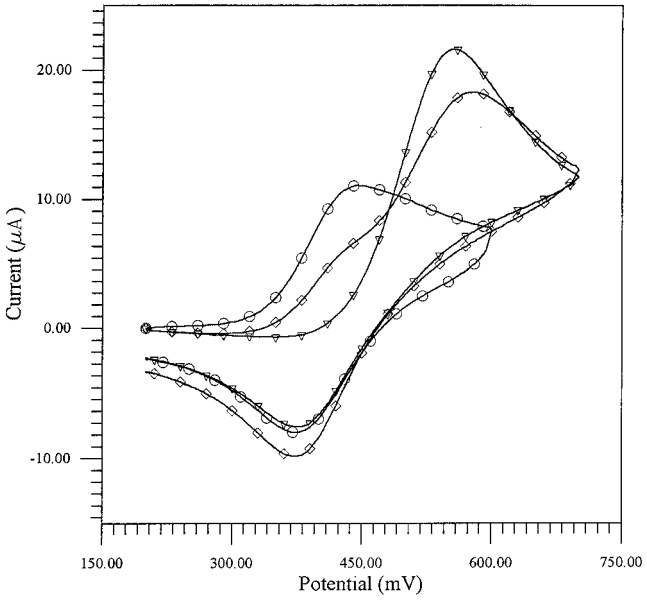

Figure 14. Cyclic voltammograms of various Cu(I) species in pH 3 buffer (0.1 M $NaBF_4$, glassy carbon electrode *vs* Ag/AgCl, saturated NaCl): (a) **9** (△), (b) **9** + TTCN (□), (c) **1** (○).

as that for **1**. This suggests that the Cu(II) ligands must be either the same or similar in both cases. If excess TTCN is added to a solution of **9**, then TTCN is seen to displace some of the TTCNO ligand, resulting in a split oxidation wave.

The ^{1}H NMR spectrum of **9** as well as that of uncomplexed TTCNO is shown in Figure 15. Since the spectrum of **9** is the same as that obtained by superposition of the spectra of uncomplexed TTCNO and a 1:1 mixture of Cu(I) and TTCN, it appears that TTCNO does not bind to $[Cu^I(TTCN\text{-}\kappa^3)]^+$ in CD_3CN solution. The TTCNO ligand is apparently replaced by acetonitrile. Thus TTCNO is a much poorer monodentate ligand[42] than TTCN or acetonitrile toward $[Cu^I(TTCN\text{-}\kappa^3)]^+$. The poor ligand character of TTCNO compared to TTCN is also demonstrated by the cyclic voltammetry of $[Cu^I(TTCN\text{-}\kappa^3)(TTCNO\text{-}\kappa^1)]$ in the presence of free TTCN as shown in Figure 14b. The appearance of an anodic wave corresponding to that of $[Cu^I(TTCN\text{-}\kappa^3)(TTCN\text{-}\kappa^1)]$ clearly suggests a CE process in which the electron transfer is preceded by the substitution of ligated TTCNO by the free TTCN added to the solution.

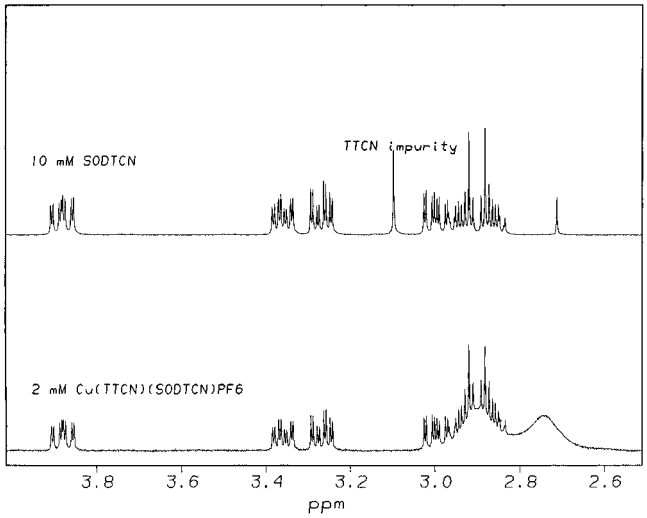

Figure 15. ^{1}H NMR spectra of (a) TTCNO and (b) **9** in CD_3CN.

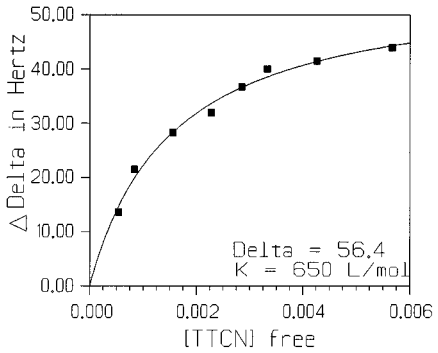

Figure 16. Binding constant graph for the binding of monocoordinated TTCN to **1** according to a procedure given in ref 26.

As pointed out above, **3** either is formed by oxidation of **1** with loss of the monodentate TTCN ligand or this ligand dissociates first and **10** is oxidized. The relative importance of these two pathways depends in large part on the relative concentrations of **1** and **10**. These concentrations depend on the binding constant for monodentate TTCN to $[Cu^I(TTCN\text{-}\kappa^3)]^+$. Although this binding constant could not be determined in water alone, it could be measured in aqueous acetonitrile by ^{1}H NMR spectroscopic monitoring of the titration of $[Cu^I(CH_3CN)_4]PF_6$ with TTCN or of $[Cu^I(TTCN)_2]PF_6$ with $[Cu^I(CH_3CN)_4]PF_6$. From the dependence of the chemical shift difference between bound and unbound TTCN on the concentration of TTCN shown in Figure 16 a binding constant of 650 L/mol can be derived[26] for the association of monodentate TTCN with $[Cu^I(TTCN\text{-}\kappa^3)]^+$. This binding constant means that $[Cu^I(TTCN\text{-}\kappa^3)L]^+$, L = H_2O or CH_3CN, and TTCN are the preponderant species at an initial concentration of **1** of 5×10^{-5} M as used in the pulse radiolysis experiments. This argues for the formation of **3** principally by oxidation of **10**. However, this binding constant may be significantly greater in water than in aqueous acetonitrile resulting in a greater importance of the formation of **3** by oxidation of **1** followed by loss of the monodentate TTCN ligand. The fact that attachment of a "soft" sulfur ligand to the "soft" Cu^+ in the unoxidized complex provides such a highly labile system serves as a convincing

(42) That TTCNO is a poorer monodentate ligand than TTCN with Cu(I) is unexpected because of the known importance of ligand π-acidity for complexes of TTCN with low valent transition metal ions[6,43] and TTCNO should be a better π-acid than TTCN.

(43) Blake, A. J.; Holder, A. J.; Hyde, T. I.; Schröder, M. *J. Chem. Soc., Chem. Commun.* **1989**, 1433.

rationale for an even weaker interaction with the "hard" Cu^{2+} and monodentate TTCN which is compatible with this case.

Correlation of Electrochemical and Pulse Radiolysis Studies. As already pointed out, the metastable intermediate formed on electrochemical oxidation of **1** and the transient precursor of **2** obtained by •OH-induced oxidation of **1** are suggested to be the same species, namely **3**, based on their similar properties. However, the conversion of this species into **2** depends on the concentration of **1** in the pulse radiolysis experiment but *not* in the electrochemical experiment. This major discrepancy may be explained on the basis of reaction and diffusion kinetics and the specific characteristics of the two techniques.

In pulse radiolysis only a small fraction (typically only a few percent at most) of the solute molecules are converted in a redox process and, furthermore, any TTCN released from the oxidized copper can freely diffuse into the bulk of the solution. Conversion of the transient **3** to **2** will, therefore, almost exclusively occur by encounter with an unoxidized Cu^+ complex (or free TTCN). In electrochemistry, it can be anticipated that all Cu^+-complexed molecules formed at the electrode surface will be oxidized in a fast and efficient electron-transfer process so that the double layer volume and immediate vicinity of the electrode become depleted of intact **1** but may still contain a high concentration of those (TTCN-κ^1) ligands which are detached from the copper in the oxidation process. This facilitates reattachment of the latter to the intermediate **3** which is presumed to exist also in electrochemistry. It also explains its independence from the Cu^+ complex concentration. The comparatively high free TTCN concentration near the electrode would also allow fast reconstitution of **1** after a possible and presumably fast reduction of any intermediate **3**, providing the rationale for reversibility irrespective of the actual stoichiometry of the copper(II) complex.

Conclusion

In conclusion, a consistent picture has emerged on the oxidation mechanism of **1** to **2** accommodating the results of a variety of complementary experimental techniques. It also includes higher pH regions in which the initial copper(I) complex appears to be partially hydrolyzed. The transient **3** formed on oxidation of **1** and which serves as the immediate precursor to **2** is $[Cu^{II}(TTCN\text{-}\kappa^3)(H_2O)_3]^{2+}$. Depending on pH, it undergoes one or more deprotonations. The structure of these hexacoordinate transients is likely to be octahedral. This replaces the previous suggestion, which was the simplest interpretation of the electrochemical data, that this species is tetrahedral $[Cu^{II}(TTCN\text{-}\kappa^3)(TTCN\text{-}\kappa^1)]^{2+}$. The key features of the mechanism for this oxidation proposed in this paper are the high lability of monodentate TTCN and the pH dependence of this process. This study shows the value of using complementary experimental techniques for discerning the chemistry of complex systems.

Acknowledgment. Partial support of this work by NATO Research Grant No. 910917 is gratefully acknowledged. S., R.S.G., and G.S.W. thank the U.S. National Institutes of Health (Grant HL-15104) for financial support of this work. Part of this work was supported by the Office of Basic Energy Sciences of the Department of Energy and, as such, it is contribution No. NDRL-3919 from the Notre Dame Radiation Laboratory. We thank Dr. Fusao Takusagawa for his assistance in the X-ray crystallographic structure determinations.

Supporting Information Available: Table of crystal data, experimental details, tables of fractional coordinates and thermal parameters, and complete listings of bond distances, bond angles, selected torsion angles, ORTEP drawings of the molecules, and PLUTO stereoviews of the unit cells for **7** and **9** (29 pages). See any current masthead page for ordering and Internet access instructions.

JA9627757